Discriminative mapping of geological formations and silica-rich zones using ASTER images: A case study of Ardakan area, Iran

Mohammad Hosein Mokhtari

Faculty of Natural Resources, Yazd University, Yazd, Iran

* Corresponding Author: Mokhtari.mh@gmail.com

Received: 01 September 2014 / Accepted: 07 October 2015 / Published online: 25 February 2015

Abstract

The Kalut-e-Ashrafa area is located in the north-east of Ardakan area in central Iran, Yazd province. This area promises copper mineralization. The most of the minerals in this study area are silica-rich veins and veinlets. Therefore, in order to identify geological formations with silica zones and to determine potential mineralization areas, ASTER images and remote sensing methods were used. Advanced Space-borne Thermal Emission and Reflection radiometer (ASTER) images helped to make discriminative maps of those geological formations and to spot silica rich zones in that area. For this purpose, Color-Ratio-Composite (CRC), False Color Composite (FCC) images of band4/band1 (Red), band3/band1 (Green), and band12/band14 (Blue) ratios were employed to enhance the FCC images and make them more distinctive, a decorrelation stretch procedure was applied to CRC images. Discrimination of silica-rich zones was performed using Matched Filtering methods applied to ASTER spectral bands. Geological formations were distinguishable in the FCC images of the study area, and the sand dunes were distinctive in the images with bluish pixels. Also, setting a threshold of x+2s on the digital numbers of the MF rule images provided implication that red areas had a high probability of being silica-rich zones.

Keywords: ASTER, Color-ratio-composite, Remote sensing, Matched filtering, Ardakan.

1–Introduction

Conventionally, mineral exploration requires ground-based geological investigation. This investigation relies on visual identification, sample collection and laboratory tests which are costly and time-consuming. Owing to advancement of satellite imagery and computer science, field surveys have been largely replaced by cost-effective remote sensing techniques (Wenk and Bulakh, 2004). In addition, broad spatial and spectral coverage characteristics of multispectral satellite data have increasingly led researchers to use remote sensing techniques to identify mineral types and their locations. Beside the production of various satellite data, several remote sensing techniques such as training and non-training methods have also been developed to explore potentially high mineralization areas. In non-training methods, satellite images are analyzed based on theoretically known interactions between electromagnetic spectra and mineral composites. However, in training methods, user-defined training points in images are presented to cluster pixels into classes corresponding to training points.

These methods have been used by several researchers, and the results have been evaluated by field observation. Among non-training methods, Principal Component Analysis (PCA), Band Rationing (BR), Least Square Fit (LS-Fit)

and False Color Composite (FCC) are the most widely used methods in mapping of hydrothermal potential alteration zones. Detecting gold mineralization zones (Asadi 2000; Souza Filho *et al*. 2003), identifying clay and iron oxide aggregations (Ezzati *et al*., 2014), and mapping alteration zones associated with porphyry copper (Honarmand *et al*., 2011) are the examples of using remote sensing data and the above-mentioned methods.

In this study, the remote sensing technique was used for two purposes: 1) discriminative mapping of geological formations, and 2) spotting silica rich zones. The remotely sensed data used in this study refer to a scene of Advanced Spaceborn Thermal Emission and Reflection Radiometer(ASTER) sensor which is on the platform of Terra satellite launched by National Aeronautics and Space Administration(NASA) in 1999 (Rencz, 1998). ASTER has three optical imaging subsystems with 14 multispectral channels (i.e. bands) functioning within Visible Near Infrared(VNIR) (3 bands), Short-Wave Infrared(SWIR) (6 bands), and Thermal Infrared(TIR) (5 bands) wave lengths regions, representing spatial resolutions of 15 m, 30 m, and 90 m respectively (Corrie *et al*., 2011). Figure 1 demonstrates band 1 of the ASTER scene of the Ardakan area, in which a 478×252 (pixels) subset has been extracted for further spectral processes.

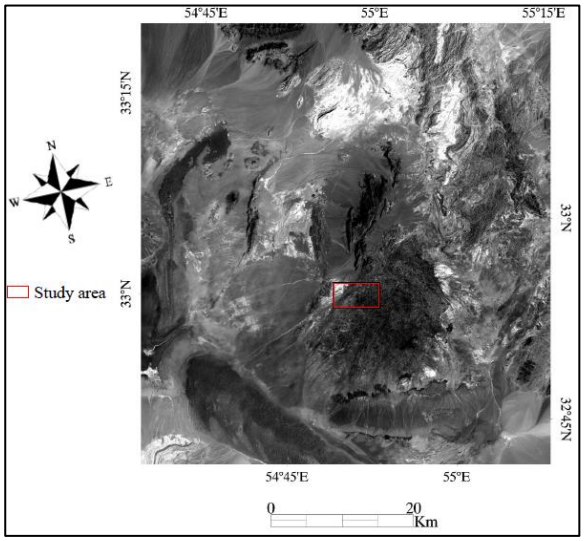

Figure1) Band 1 of ASTER scene of the study area.

Previous pieces of research on the Ardakan area were completed by Mokhtari *et al*. (2014). In this study, an area prone to Cu mineralization has been considered for geochemical exploration on the scale of 1:25,000 using sediment samples from stream channels. The results of the study show that important Cu anomalies in this area are very closely matched with quartz veins and mineralized outcrops.

2-Geology of the study area

The study area is located in the north-east of Yazd, Iran, somewhere within 32.54 and 33.00 N and 54.50 and 55.00 E (Fig.2). Due to the dry climate, vegetation in this area is limited. Shale and sandstone are the most important units of geology in this area. Figure 3 presents a geological map of the area with its known mineralization veins. The basic unit in the area is mostly composed of layers of sandstone and siltstone, but the other units are the ones found scattered over the area.

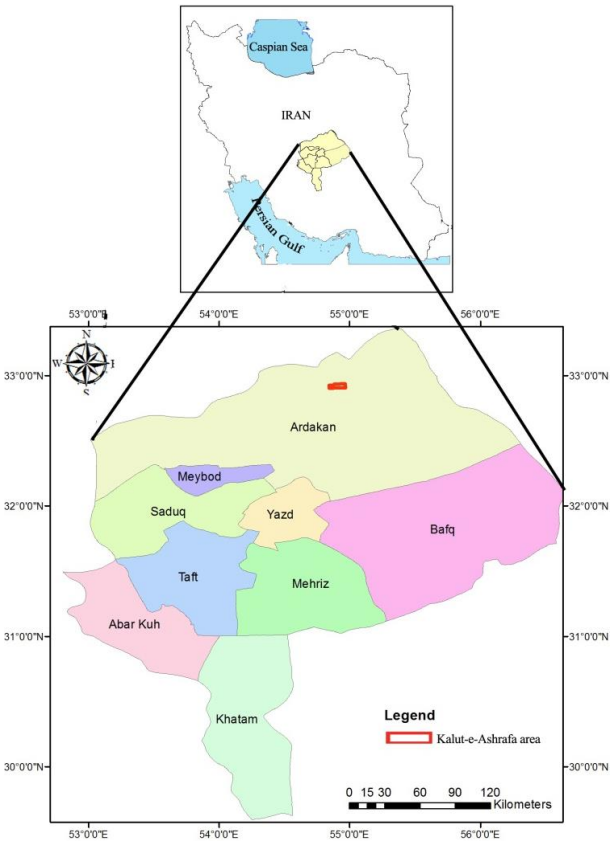

Figure 2) Location of the Kalut-e-Ashrafa area in Yazd province.

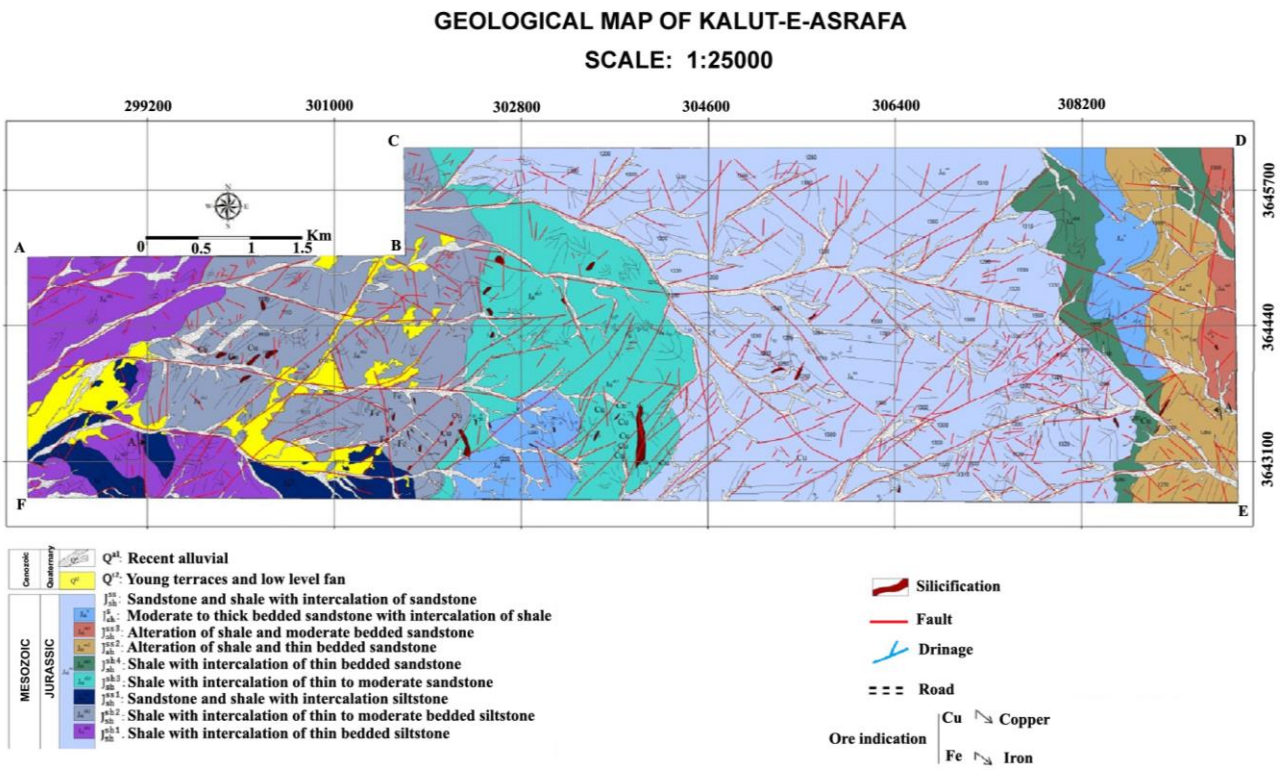

Figure 3) Geological map of the study area with known mineralization veins (Mokhtari et al., 2014).

The basic unit actually includes higher rocky outcrops in the center of the area. The highest points in the mountain range consist of thick sandstone associated with shale layers as another version in the unit. . Shale layers are not pure and contain small lenses of sandstone. In the eastern parts of the unit, silica veins associated with copper mineralization can be observed.

Silica veins injection was done to fault breccia, fractures associated with faults and stretching joints related to folds. Among silica vein types, those associated with faults are specially significant and potential for mineralization. The veins in the silica zone range from 35 to 630 meters in length and from5 to 30 meters in width. Most of the veins in the silica zones have a Northeast-Southwest stretch. Copper mineralization was made multi-step along with silica veins injection. The most important mineral in the study area is in the form of veins and veinlets controlled by fault zones.

The oldest rock unit in the area is shale with thin layers of silt and sandstone stretching from NE to SW. Indeed, this is one of the most important units in the Kalut-e-Ashrafa that hosts many quartz veins and copper minerals.

The unit, located in the west part of the explored area, has copper minerals disseminated within many quartz-hematite veins with the maximum thickness of one meter and length of several meters. Layers of sandstone associated with these minerals are medium in size. Several faults in these units have smashed the rocks and opened spaces through which ore-bearing fluid passes. This has ultimately caused the formation of quartz veins associated with copper mineralization in these structures. Although most of the veins cut through the host rocks (i.e. shale and sandstone Shemshak formation), the weakness of layers at the interface between shale and sandstone has led to a peripheral expansion. Consequently, this lithological structure has a significant role in the distribution of ore-bearing fluid in the region (Fig. 4).

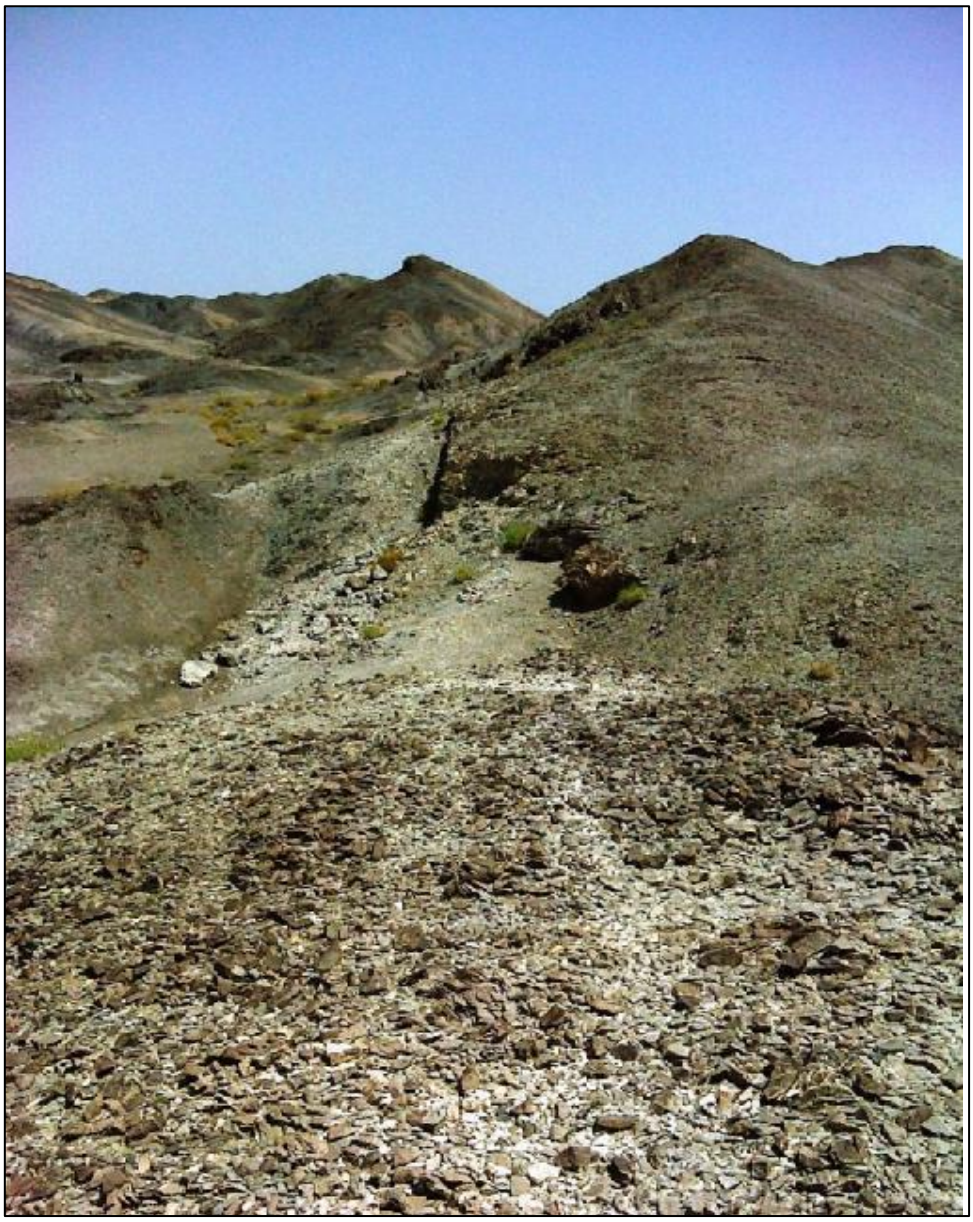

Figure 4) Silicic veins.

3-Materials and methods

3.1- Satellite data and preprocessing

The data obtained from TERRA ASTER sensors were used to discriminatively map the geological formations and to spot the silica-rich zones. ASTER cloud-free level 1B satellite data taken on Sep 4, 2001 were obtained from NASA Land Processes Distributed Active Archive Center (LP DAAC). Level 1B data, the recorded radiance at the sensor ($Wm^{-2}sr^{-1}\mu m^{-1}$), are produced from level 1A by applying a radiometric coefficient. ASTER data characteristics are shown in Table 1.

Table1) Characteristics of three ASTER sensor systems (Thome, Palluconi et al. 1998).

Subsystem	Band No.	Wavelength µm	Pixel size	Quantization level
Visible-near infrared	1	0.52-0.60	15m	8
	2	0.63-0.69		
	3N	0.78-0.86		
	3B	0.78-0.86		
Shortwave infrared	4	1.600-1.700	30m	8
	5	2.145-2.185		
	6	2.185-2.225		
	7	2.235-2.285		
	8	2.295-2.365		
	9	2.360-2.430		
Thermal-infrared	10	8.125-8.475	90m	12
	11	8.475-8.825		
	12	8.925-9.275		
	13	10.25-10.95		
	14	10.95-11.65		

In order to eliminate any kind of atmospheric effects before image analysis or information extraction, radiometric and atmospheric calibration is necessary (Mather, 1997). Radiometric and atmospheric corrections were performed on the ASTER data of this study using the Log Residuals calibration method. This transformation creates a pseudo reflectance image that is useful for analyzing mineral-related absorption features.

The image was geo-registered to the Universal Transverse Mercator (UTM) World Geodetic System1984 (WGS84) zone 40 coordinate system by using 30 ground control points. First-order polynomial transformation with the nearest neighbor re-sampling method was applied to the images to fit the image coordinates to the coordinates of the ground control points. An overall root mean square error of less than 0.28 pixels was achieved.

4-Materials and methods

4.1- Discriminative mapping

In order to do the discriminative mapping of the geological formations, the band rationing method was used. In a band rationing process, the pixels in one image are divided by the corresponding pixels in another image. This provides relative band intensities and, as a result, the spectral differences of bands are enhanced. In addition, three ratios can be combined into a color-ratio-composite (CRC) to determine the approximate spectral shape of the pixels spectrum. A False Color Composite (FCC) image of band4/band1 (Red), band3/band1 (Green), and band12/band14 (Blue) ratios was used to map the geological formations of the study area. To enhance the FCC image and make it more distinctive, a decorrelation stretch procedure was applied to it. It is very useful in these conditions, in which there are highly correlated bands (i.e. bands 1, 3, and 4 from SWIR) (Aleks. *et al*. 2004).

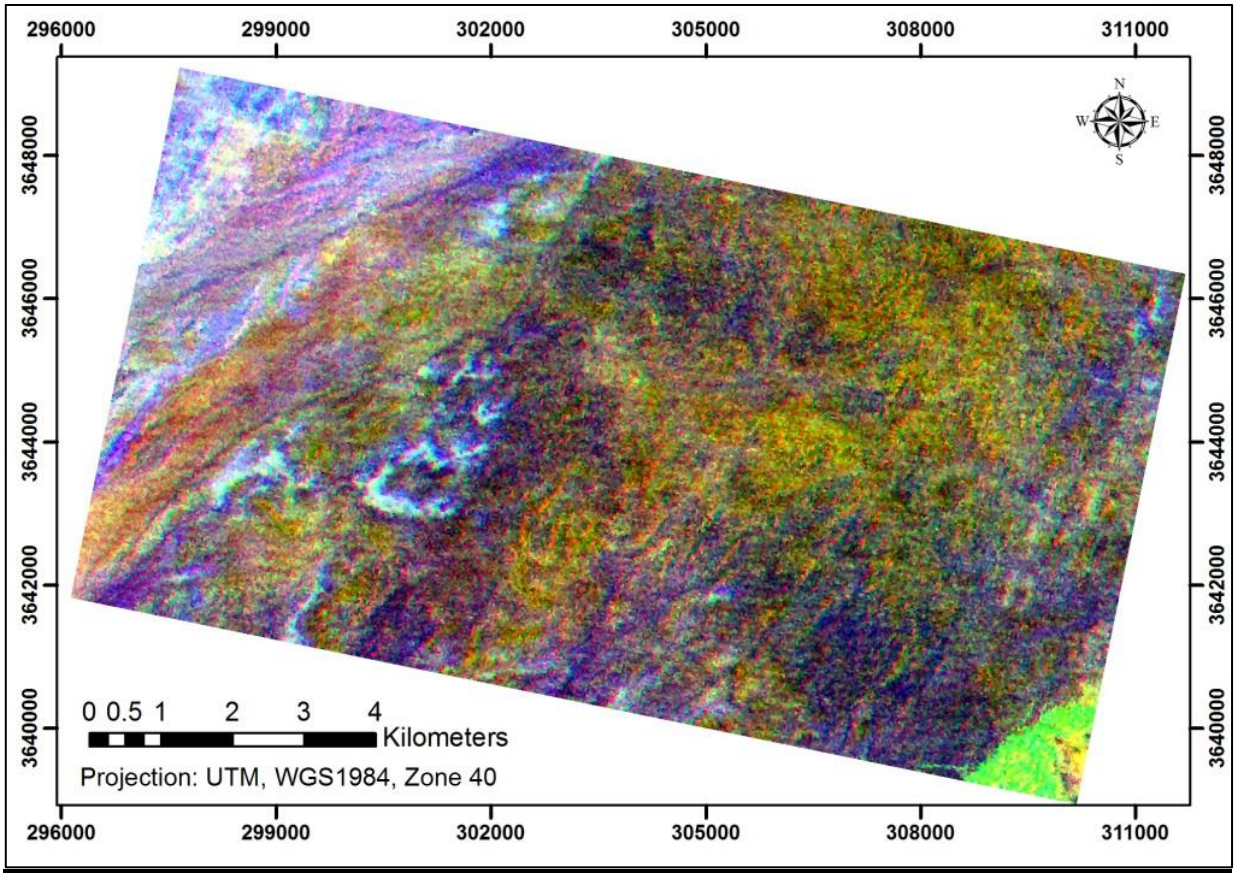

Figure 6) False Color Composite of the study area with band4/band1 (Red), band3/band1 (Green), and band12/band14 (Blue) ratios.

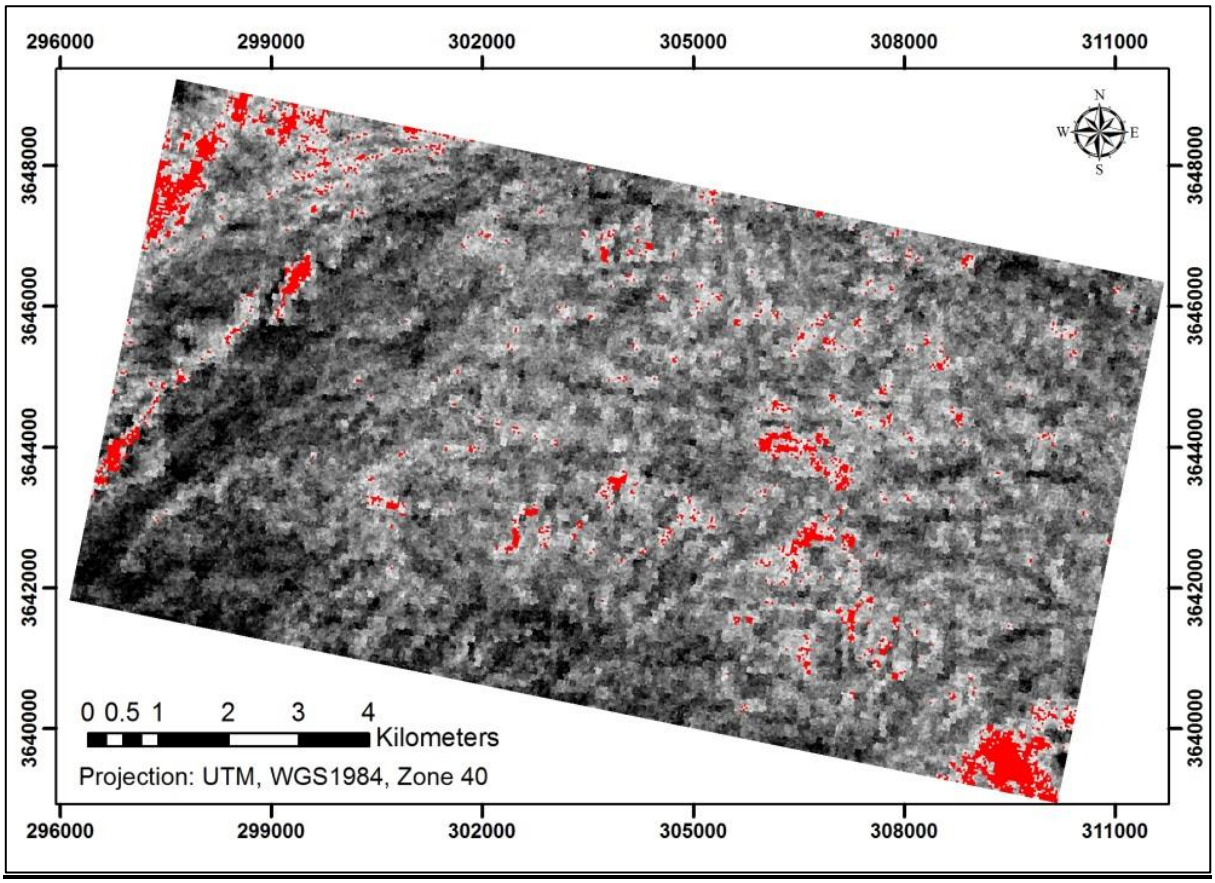

Figure 7) MF rule image of Quartz end member to indicate the silica-rich zones. Red pixels refer to the threshold of x+2s applied on the scene.

The decorrelation stretch is also known as an effective method for extracting information from multi-spectral thermal-infrared bands. In the decorrelation stretch process, three bands are used as input. For the image decorrelation process, the following four steps are performed. First, the covariance matrix is determined and the eigenvectors are calculated. Then, the image is transformed from the radiance domain to the principal component space. As the third step, the principal component images are stretched in order to equalize the variance of images with the highest signal to noise ratios. In the final step, the principal component images are transformed to the original radiance space (Gillespie, 1992).

4.2- Mapping the silica-rich zones

Matched Filtering (MF) mapping method was used to map the silica-rich zones. MF is a technique for spectral unmixing of only user-defined end members of the spectral mapsand can be used in multi-spectral and hyper-spectral remote sensing(Borengasser*et al*., 2007).

This method minimizes the response of the composite unknown background while it maximizes the response of the known end member, hence matching the known signature (e.g. silica-rich zones) (Borengasser *et al*., 2007). MF can find spectral signatures of materials which constitute even a relatively minor fraction of the spectral content within the image (Borengasser *et al*., 2007). To do so, the United States Geological Survey (USGS) spectral library for minerals was re-sampled to the ASTER scene of the study area, and the Quartz spectral plot was then used in the MF mapping procedure as the end member to produce the abundance map of the silica-rich zones.

The mentioned FCC image of the study area is shown in Figure5, in which the geological formations are now very distinguishable. Overlaying the FCC image on the geological map of the zone (Fig. 2) reveals that the sand

dunes are distinctively well, which is shown in bluish pixels of Figure5. The Figure6 demonstrates the gray-scale rule image of the silicic areas, where the lighter the pixels are, the purer they are and the more they represent the silicic zones. Setting a threshold of x+2s on the digital numbers of the MF rule image generated the red Regions of Interest (ROI) areas, implying the high occurrence probability of silica-rich regions.

5-Conclusion

In this research, discriminative mapping of the geological formations and spotting of the silica-rich zones were done in the study area using Advanced Space-borne Thermal Emission and Reflection radiometer (ASTER) images. By this method, The successful delineation of the geological-structural units was conducted in the Kalut-e-Ashrafa area in Yazd province. The most important mineralization in the study area is in the vein– veinlet form which is controlled by fault zones. Copper mineralization is disseminated within many quartz-hematite veins with the maximum thickness of one meter and length of several meters. Quartz veins associated with copper mineralization are located on shale units within medium layers of sandstone. Copper mineralization has been hosted by quartz veins which are formed inside the fractures. These structures are highly important for recognition and delineation of mineral zones. A different technique was applied on ASTER images in order to recognize the geological features of the area. Matched Filtering method was used on ASTER spectral bands to identify the silica-rich zones. Finally, a False Color Composite analysis showed the geological formations of the study area very distinguishably. In the images obtained, the sand dunes are distinctive with bluish pixels, and the gray-scale rule image of the silicic areas represents the silicic zones. Setting a threshold of x+2s onthe digital numbers of the MF rule images provided implication that red areas had a high probability of being silica-rich zones.

Acknowledgments:

The authorDr. S.Alipour and an anonymous reviewer for their appreciate comments which help him to improve manuscript.

References:

Asadi, H. H. 2000. The Zarshuran gold deposit model applied in a mineral exploration GIS in Iran. The Netherlands, University of Delft and ITC. PhD 127–165.

Borengasser, M., Hungate, W. S., Watkins, R. 2007. Hyperspectral remote sensing: principles and applications, Crc Press. 128 p.

Corrie, R., Ninomiya, Y., Aitchison, J. 2011. Applying advanced spaceborne thermal emission and reflection radiometer (ASTER) spectral indices for geological mapping and mineral identification on the Tibetan Plateau.International Archives of the Photogrammetry, Remote Sensing, and Spatial Information Science, XXXVIII: 464–469.

Souza Filho, C. R.,Azevedo, F.,Brodie, C. 2003. Targeting key alteration minerals in epithermal deposits in Patagonia, Argentina, Using ASTER imagery and principalcomponent analysis. International Journal of Remote Sensing: 24, 4233–4240.

Ezzati, A., Mehrnia, R., Ajayebi, K. 2014. Detection of Hydrothermal potential zones using remote sensing satellite data in Ramand region, Qazvin Province, Iran. Journal of Tethys: 2, 93–100.

Gillespie, A. R.1992. Enhancment of multispectral thermal inferared images: Decorrelation contrast stretching. Remote Sensing of Environment: 42, 147–155.

Honarmand, M., Ranjbar, H., Shhabpour, J. 2011. Application of Spectral Analysis in

Mapping rothermal Alteration of the Northwestern Part of the Kerman Cenozoic Magmatic Arc, Iran. Journal of Sciences: 22, 221–238.

Kalinowski,A., Oliver, S. 2004. ASTER mineral index processing manual.Remote Sensing Applications. Geoscience Australia 37.

Mather, P.,Koch, M.2010. Computer Processing of Remotely-Sensed Images: An Introduction. 4th ed. John Wiley-Blackwell, 460 p.

Mokhtari, A.R, Roshani-Rodsari, P., Fatehi, M., Shahrestani, Sh., Pournik, P. 2014. Geochemical prospecting for Cu mineralization in an arid terrain-CentralIran. Journal of African Earth Sciences: 100, 278–288.

Rencz, A., N. (Ed.) 1998. Remote Sensing for the Earth Sciences (Manual of Remote Sensing, Vol 3). Wiley and Sons, New York.

Thome, K., F. Palluconi, et al. (1998). Atmospheric correction of ASTER." Geoscience and Remote Sensing: 36, 1199–1211.

Wenk, H.-R., Bulakh, A.2004. Minerals: Their Constitution and Origin. Cambridge University Press, 666 p.